Modeling and Control of a Dual Stator Multiphase Induction Motor for Electric Vehicle Technology

M. SOWMIYA[1], G. RENUKA DEVI[2]
[1]Department of Electrical and Electronics Engineering,
Anna University, Chennai,
INDIA.
[2]Department of Electronics and Communication Engineering,
School of Engineering, JNU, New Delhi,
INDIA.

Abstract: — This paper presents the dynamic modeling and speed control of a Dual Stator Multiphase Induction Motor (DSMIM) in MATLAB/Simulink environment. The torque production and load sharing capability of the model is analyzed under free acceleration conditions when subjected to a frictional load profile. Its speed control operation is realized using the conventional V/f and vector based Indirect Field-Oriented Control (IFOC) methods. The torque and speed tracking ability of the machine with the chosen control techniques were simulated. The better dynamic performance of IFOC controlled DSMIM drive model establishes its utility in Electric Vehicles (EV) technology and research. Credibility of the proposed model in EV application is verified by testing it against the standard Modified Indian Drive Cycle (MIDC). The corresponding torque and speed waveforms obtained under the drive cycle analysis are illustrated. The proposed model well supports sudden load changes with a better load sharing competence.

Keywords: — DSMIM, d-q equivalent circuit, Dynamic model, MATLAB/Simulink, V/f control and IFOC control.

Received: March 23, 2024. Revised: September 8, 2024. Accepted: November 9, 2024. Published: December 17, 2024.

1. Introduction

Induction motors (IMs) rule the world's motor population. Single-phase IMs are extensively used in household appliances like vacuum cleaners, fans, washing machines, centrifugal pumps, blowers as it is featured with simple construction, high reliability and cheaper cost [**1-3**]. Three phase IMs are hyped in industrial utility. They are also exceedingly preferred in many of the traction applications like tram cars, metro cars, Electric Multiple Units (EMUs) and electric railway locomotives [**4-6**]. A propulsion unit in Electric Vehicle (EV) should essentially develop enough starting torque to overcome vehicle inertia and should operate at better efficiency for a wider load range [**7-9**]. Three phase IMs in EV propulsion units, are bound to inbuilt disadvantages like low power factor, efficiency drops at low loads and high input surge current. Therefore, with the stipulation of satisfying high-efficiency demands, high load demands, and longer driving range a conventional three phase IMs are subjected to renovations in their constructional arrangement [**10**]. These renovations lead to the discovery of configurations such as Multiphase Induction Motors (MIMs) and Dual Stator Winding Induction Motors (DSWIMs). MIM, whose number of phases is greater than three, gained popularity with the growth and expansion of power electronic drives [**11-13**]. Its stator windings are shifted symmetrically by 360 °/ number of phases and are designed with the idea of building an IM along with its control electronics as a single system. Reduced current per phase without increasing the voltage per phase, lower dc-link current harmonics, reduced torque pulsations, increased torque to current ratio and increased fault tolerance with reference to its three-phase counterpart are the major aspect for its wider utilization in submarines, rail traction, avionics and Electric Vehicle (EV) applications [**14-16**].

The concept of load sharing and torque producing capability headed its importance in EV with the escalation of load during drive [**17**]. The research explorations proposed a configuration that included a secondary stator winding along with the existing primary stator winding. This type of configuration is usually termed as a Dual Stator Winding Induction Motor (DSWIM) [**18, 19**]. The two sets of insulated stator windings in this configuration are wound in the same stator core and are excited separately by two inverters depending upon the load demand. This configuration affords better reliability, effective torque and speed controllability and fast dynamic response. But the presence of dual stator windings on the same stator core would magnetize the entire stator core even at lesser load demand with the excitation of any one the stator windings. This set stage for the development of more iron losses and improper stator core utilization [**20, 21**]. Therefore, it highly suffers from efficiency deterioration at light loads. Thus, to decrease harmonics, increase fault tolerance capability, increase loading capacity and energy efficiency a novel constructional arrangement with dual stators and increased number of phases is proposed. The cross-sectional view of the Dual Stator Multiphase Induction Motor (DSMIM) is shown in Figure 1. Its design includes two separate stator cores. Each consisting a symmetrical five phase star connected winding, sharing a common hollow cage rotor. The stators are excited selectively, to support the varying load torque demands. During the excitation the individual stator core magnetization will greatly reduce the iron losses and improve efficiency. Thus, an EV propulsion unit encompassing DSMIM is expected to exhibit an energy efficient performance at various operating points. It is also benefited with the features of IM, DSWIM and MIM. A sensible selection of controller will effectively reduce the complexity of the traction unit and improves its performance characteristics. V/f and Indirect field-oriented control (IFOC) are the widely utilized speed control techniques in many of the traction units [**22-24**]. Vector Control allows a precise and wide control over speed at all four quadrants.

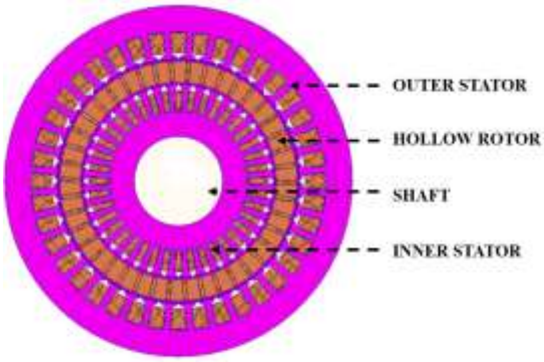

Figure 1. Cross-Sectional view of DSMIM

Direct vector control methods are more advanced and respond ten times faster than indirect vector control methods but it involves flux or torque sensors that add complexity and cost on implementation. Considering this as a major constraint, the implementation of a direct vector control method loses credibility in many industrial and traction applications [**25, 26**]. In IFOC the rotor position is premeditated from the speed feedback. This eliminates the problems associated with the flux sensors as they are absent. This control method is characterized by an improved torque response, dynamic speed accuracy, Short-term overloading capability, precise low-speed operation, reduction of motor size, cost and power consumption. These properties establish the utility of IFOC in EV application.

An EV driving pattern commonly known as a drive cycle is characterized by acceleration, cruising, coasting and braking. It is built with reference to the real time road and traffic conditions. Drive cycle analysis assist in energy efficiency calculations at different stages of the driving pattern to predetermine EV's net energy requirement [**27, 28**].

The paper is organized to present the dynamic model of DSMIM in section 2. Its load sharing analysis and its results under free acceleration condition are illustrated in section 3. Speed control analysis of the drive is carried out with the conventional v/f open loop controller, v/f closed loop controller and a vector based IFOC. Its torque and speed tracking capability are illustrated through the results in section 3

2. Dynamic Modeling of DSMIM

Transient analysis and high-performance drive control, such as vector control is initiated by the development of a dynamic model [**29, 30**]. DSMIM modelling necessitates the consideration of following assumptions: (i) isolated and sinusoidal distribution of stator windings, (ii) negligible saturation, (iii) negligible effect of eddy current, friction and windage losses and (iv) uniform air gaps. Since the two stators are electrically isolated two sets of d-q equivalent circuits are framed for analysis and therefore two sets of d-q modelling equations are obtained under a common reference frame. D-axis and q- axis equivalent circuit of DSMIM while exiting the outer and inner stators are represented from Figure 2 to Figure 5 respectively.

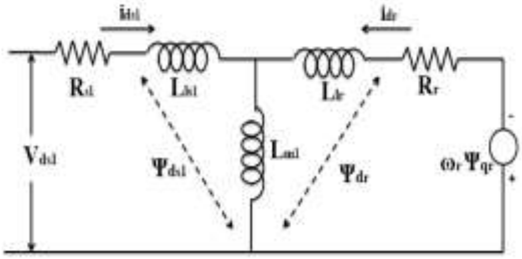

Figure 2. D- Axis Equivalent Circuit of Outer Stator

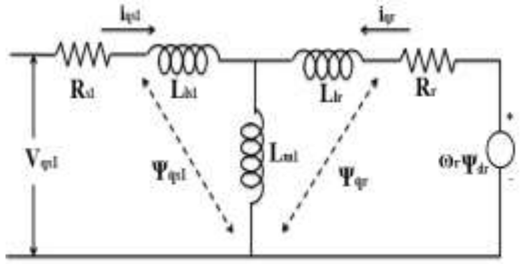

Figure 3. Q- Axis Equivalent Circuit of Outer Stator

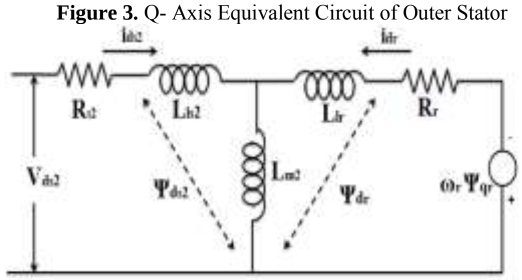

Figure 4. D- Axis Equivalent Circuit of Inner Stator

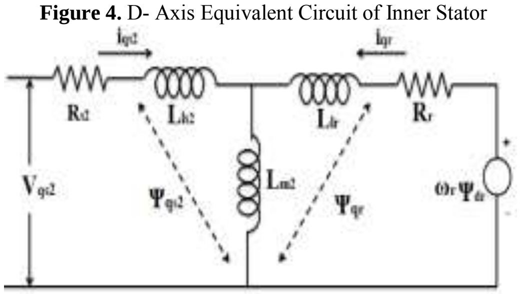

Figure 5. Q- Axis-Equivalent Circuit of Inner Stator

For simplicity in analysis the dual stator d-q voltage equations are derived under stator reference frame i.e., fixing $\theta_e = 0$. The d-q voltage equations while exciting the outer stator is given by equation (1) and equation (2) respectively.

$$V_{ds1} = i_{ds1}R_{s1} + \frac{d}{dt}\psi_{dr} - \omega_e\psi_{qs1} \tag{1}$$

$$V_{qs1} = i_{qs1}R_{s1} + \frac{d}{dt}\psi_{qr} + \omega_e\psi_{ds1} \tag{2}$$

The d-q voltage equations while exciting the inner stator is given by equations (3) and (4) respectively.

$$V_{ds2} = i_{ds2}R_{s2} + \frac{d}{dt}\psi_{dr} - \omega_e\psi_{qs2} \quad (3)$$

$$V_{qs2} = i_{qs2}R_{s2} + \frac{d}{dt}\psi_{qr} + \omega_e\psi_{ds2} \quad (4)$$

The d-q rotor voltage equations while exciting either the individual stator or while simultaneously exciting both the stators is given by equations (5) and equation (6) respectively.

$$V_{dr} = i_{dr}R_r + \frac{d}{dt}\psi_{dr} - (\omega_e - \omega_r)\psi_{qr} \quad (5)$$

$$V_{qr} = i_{qr}R_r + \frac{d}{dt}\psi_{qr} + (\omega_e - \omega_r)\psi_{qr} \quad (6)$$

The d-q flux linkage component of the stator, air gap and rotor while exciting the outer stator are represented from equations (7) to equation (12) respectively.

$$\psi_{ds1} = L_{ls1}i_{ds1} + L_{m1}(i_{ds1} + i_{dr}) \quad (7)$$

$$\psi_{qs1} = L_{ls1}i_{qs1} + L_{m1}(i_{qs1} + i_{qr}) \quad (8)$$

$$\psi_{dm1} = L_{m1}(i_{ds1} + i_{dr}) \quad (9)$$

$$\psi_{qm1} = L_{m1}(i_{qs1} + i_{qr}) \quad (10)$$

$$\psi_{dr} = L_{lr}i_{dr} + L_{m1}(i_{ds1} + i_{dr}) \quad (11)$$

$$\psi_{qr} = L_{lr}i_{dr} + L_{m1}(i_{qs1} + i_{qr}) \quad (12)$$

The d-q flux linkage component of the stator, air gap and rotor while exciting the inner stator are represented from equation (13) to equation (18) respectively.

$$\psi_{ds2} = L_{ls2}i_{ds2} + L_{m2}(i_{ds2} + i_{dr}) \quad (13)$$

$$\psi_{qs2} = L_{ls2}i_{qs2} + L_{m2}(i_{qs2} + i_{qr}) \quad (14)$$

$$\psi_{dm2} = L_{m2}(i_{ds2} + i_{dr}) \quad (15)$$

$$\psi_{qm2} = L_{m2}(i_{qs2} + i_{qr}) \quad (16)$$

$$\psi_{dr} = L_{lr}i_{dr} + L_{m1}(i_{ds2} + i_{dr}) \quad (17)$$

$$\psi_{qr} = L_{lr}i_{dr} + L_{m1}(i_{qs2} + i_{qr}) \quad (18)$$

The d-q flux linkage component of the air gap and rotor while simultaneously exciting the inner and outer stator are represented from equations (19) to equation (21) respectively.

$$\psi_{dm} = \psi_{dm1} + \psi_{dm2} \quad (19)$$

$$\psi_{qm} = \psi_{qm1} + \psi_{qm2} \quad (20)$$

$$\psi_{dr} = i_{dr}(L_{lr} + L_{m1} + L_{m2}) + i_{ds1}L_{m1} + i_{ds2}L_{m2} \quad (21)$$

The d-q components of the outer stator current are obtained by equation (22) and equation (23) respectively.

$$i_{ds1} = \frac{\psi_{ds1}(L_{lr} + L_{m1}) - L_{m1}\psi_{dr}}{(L_{ls1}L_{lr} + L_{ls1}L_{m1} + L_{m1}L_{lr})} \quad (22)$$

$$i_{qs1} = \frac{\psi_{qs1}(L_{lr} + L_{m1}) - L_{m1}\psi_{qr}}{(L_{ls1}L_{lr} + L_{ls1}L_{m1} + L_{m1}L_{lr})} \quad (23)$$

The d-q components of the inner stator current are obtained by equation (24) and equation (25) respectively.

$$i_{ds2} = \frac{\psi_{ds2}(L_{lr} + L_{m2}) - L_{m2}\psi_{dr}}{(L_{ls2}L_{lr} + L_{ls2}L_{m2} + L_{m2}L_{lr})} \quad (24)$$

$$i_{qs2} = \frac{\psi_{qs2}(L_{lr} + L_{m2}) - L_{m2}\psi_{qr}}{(L_{ls2}L_{lr} + L_{ls2}L_{m2} + L_{m2}L_{lr})} \quad (25)$$

Later the d-q stationary current components of the two stators are converted into its equivalent five phase components using Inverse Clark's transformation. The rotor d-q currents developed under dual stator excitation is given by equations (26) and equation (27) respectively.

$$i_{dr} = \frac{\psi_{dr}(L_{lr} + L_{m1} + L_{m2}) - L_{m1}\psi_{ds1} - L_{m2}\psi_{ds2}}{L_{lr}(L_{ls1} + L_{ls2} + L_{m1} + L_{m2}) + L_{m1}L_{ls1} + L_{m2}L_{ls2}} \quad (26)$$

$$i_{dr} = \frac{\psi_{qr}(L_{lr} + L_{m1} + L_{m2}) - L_{m1}\psi_{qs1} - L_{m2}\psi_{qs2}}{L_{lr}(L_{ls1} + L_{ls2} + L_{m1} + L_{m2}) + L_{m1}L_{ls1} + L_{m2}L_{ls2}} \quad (27)$$

Under mode I the net electromagnetic torque T_{e1} is developed by exciting the outer stator. It is given by equation (28)

$$T_{e1} = PL_{m1}[i_{qs1}i_{dr} - i_{ds1}i_{qr}] \quad (28)$$

Under mode 2 the net electromagnetic torque T_{e2} is developed by exciting the inner stator. It is given by equation (29)

$$T_{e2} = PL_{m2}[i_{qs2}i_{dr} - i_{ds2}i_{qr}] \quad (29)$$

Stator	Inner Stator	Outer Stator
Rated Power (P)	2 HP	9 HP
Rated Current (I)	2 A	11A
Stator Resistance (R_s)	10 Ω	1.47 Ω
Stator Leakage Inductance (L_{ls})	0.04 H	1.834 H
Rotor Resistance (R_r)	6.3 Ω	1.393 Ω
Rotor Leakage Inductance (L_{lr})	0.04 H	1.834 MH
Magnetizing Inductance (L_m)	1.05 H	0.139 H
Rotor		
Rotor Frictional constant (B)	0.03Kgm^2	
Rotor Inertia (J)	0.0015Nms	

Table 1. DSMIM Parameters

Under mode 3 the net electromagnetic torque T_e is developed by the algebraic addition of the torques produced on exciting the outer and inner stator since both the stator windings are excited by a synchronized power supply. The torque equation under this mode is given by equation (30).

$$T_e = T_{e1} + T_{e2} \tag{30}$$

The speed ω_m developed by the rotor is given by the equation (31).

$$\omega_m = \int \frac{P}{2J}(T_e - T_l)dt \tag{31}$$

With the above equations dynamic model of a Dual stator Five Phase Induction Motor is developed in MATLAB/ Simulink. The developed model could further be fitted in the analysis of its free acceleration characteristics and load characteristics.

3. Free Acceleration Characteristics of DSMIM

The DSMIM considered for case study is of 11 HP rated power, 5 phase, 230 V per phase, 50 Hz, 4 pole and 1440 rpm. The 9HP outer stator excitation supports a rated load demand of 44 Nm and the 2 HP inner stator excitation supports a rated load demand of 8 Nm. A synchronized excitation of the dual stators supports a net load demand of 52 Nm.

The five phase modelling parameters used for the analysis were taken from the two, three phase IM modeling parameters in [**31, 32**]. The magnetizing inductance developed while exciting the five-phase winding set is calculated from equation (32).

$$L_{m(5\Phi)} = \frac{n}{2} L_{m(3\Phi)} \tag{32}$$

Thus, the machine parameters used for dynamic modeling are listed in Table 1.

The dual five phase stator windings are supplied by two separate and identical five phase neutral leg Voltage Source Inverters (VSIs). The VSIs are made to operate under the same operating conditions as listed in Table 2.

Table 2. Voltage Source Inverter Parameters

Input voltage (V_{dc})	560 V
Average input current (I_{dc})	2.2 A
No. of legs	5
Modulation index (MI)	0.8
Operating frequency (f_r)	50 Hz
Switching frequency (f_s)	10 K Hz

Sinusoidal Pulse Width Modulation (SPWM) technique is used in the pulse generation of both the five phase VSIs. The SPWM technique used in the simulation study is exhibited in Figure 6.

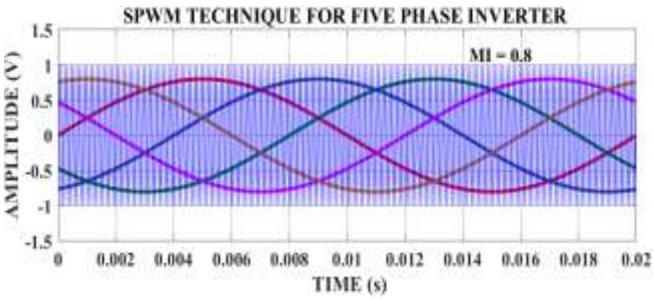

Figure 6. SPWM Pulse Generation

A triangular carrier of amplitude 1V is compared with five sinusoidal references of which are phase shifted by 72^0 [**33, 34**]. The amplitude of the sinusoidal reference is fixed with the value equal to the modulation index i.e., 0.8 V. It is important to maintain a common switching frequency for the two inverter switches in order to synchronize their switching pattern [**35**]. This condition synchronizes the flux generated during the dual stator excitation and hence torque generated by them.

Dynamic model of DSMIM is developed and made to operate at its rated load demand. Excitation to the dual stator windings is provided by the VSIs modeled above. The per phase voltage developed by the 5 phase VSI is shown in Figure 7.

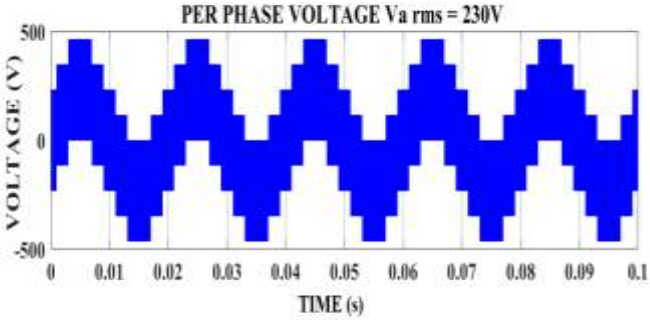

Figure 7. Five Phase Stator Voltage

A voltge of 230 V RMS is generted at the output of the inverters. For the case of identifying the percentage of Total Harmonic Distorsion (THD) in the generated voltage waveform, Fast Fourier Transform (FFT) analysis is carried out through the simulation. The THD window developed for one complete cycle of the per phase voltage V_a and it is depicted in Figure 8.

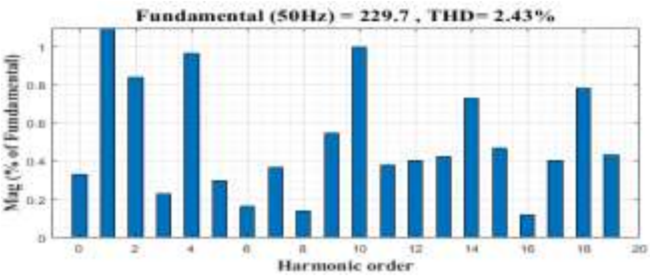

Figure 8. Speed Tracking of open loop V/f Controlled DSMIM

The THD in the voltage waveform is identified to be 2.34%. This harmonic content is expected to effect in lesser ripple content in the torque and speed waveforms at the output. The stator current, torque and speed waveforms developed by the simulation are analyzed. The stator current developed at the outer and inner stator windings are shown in Figure 9 and Figure 10 respectively.

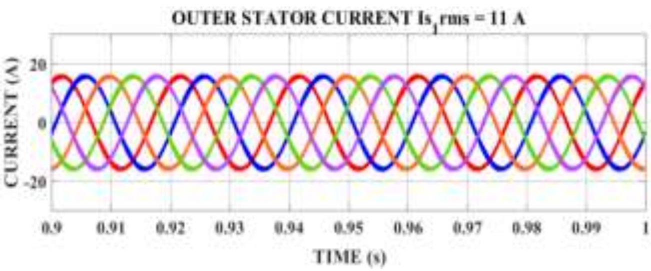

Figure 9. Five Phase Outer Stator Current

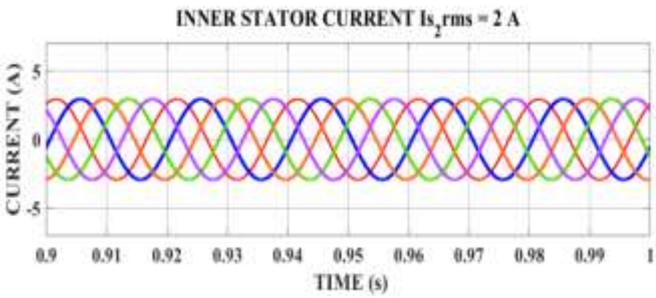

Figure 10. Five Phase Inner Stator Current

From Figure 9 and Figure 10 it is noticeable that under rated load demand, the excitation of outer stator winding and inner stator winding produces five phase currents of 11A rms and 2A rms respectively.

Study on load sharing between the stators are made by testing the model under 10%, 25%, 75% and 100% of the full load demand. The torque developed by the outer stator and the inner stator is depicted in Figure 11 and Figure 12 respectively. The net torque developed by DSMIM is depicted in Figure 13. Speed developed during this rated load condition is depicted in Figure 14.

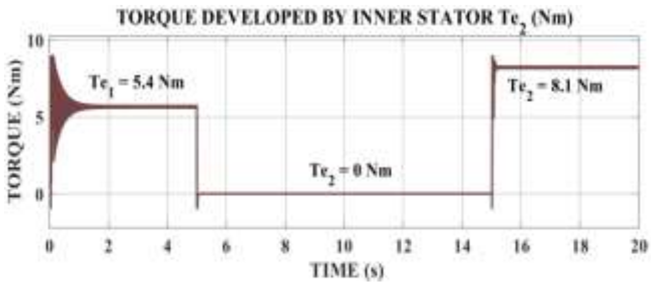

Figure 11. Torque Developed by Inner Stator at Rated Load Demand

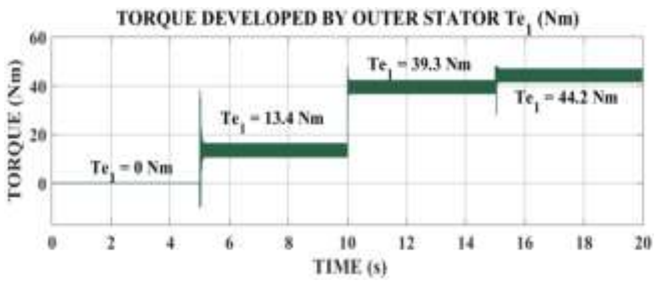

Figure 12. Torque Developed by Outer Stator at Rated Load Demand

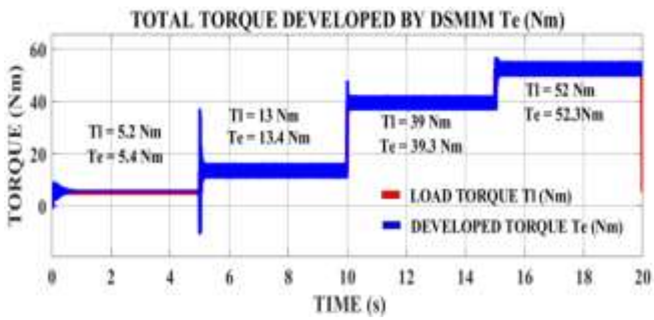

Figure 13. Net Torque Developed by DSMIM at Rated Load Demand

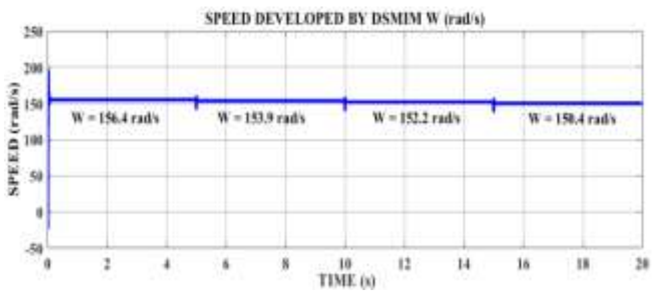

Figure 14. Speed Developed by DSMIM at Rated Load Demand

It is observed from Figure 11 and Figure 12 that during 10% of total load demand that is during the time interval between 0s and 5s only the inner stator is excited to generate torque and the outer stator is kept unexcited. Once when the load demand rises at 5s to 25% which is greater than the full load torque developed by the inner stator, the excitation now shifts to the outer stator developing torque during the time interval between 5s and 10s. When the load demand further rises to 75 % and full load, both the stators are excited to develop torque that gets algebraically added and satisfies the net load demand during the interval between 10s and 20s.

Figure 13 depicts the total torque developed by the DSMIM tracks the applied load torque with a torque ripple of 15.8 %. Figure 14 shows the speed developed by the DSMIM which gradually decreases with the increase in load demand. It is also noticeable that the load sharing between the stators is based on the power rating of the machine under individual stator excitations. The outer stator and the inner stator in the model contribute to 85% and 15% of the total load demand respectively.

4. Speed Control of DSMIM

IM speed control is quite challenging as its rate of change of speed is very low for its entire loading range. The V/f controlled DSMIM drive and IFOC controlled DSMIM drive were analyzed by providing a desired speed pattern of 25% of rated speed followed by 50%, 100% and 75% of the rated speed at regular time intervals of T= 1 s. The load demand patterns were chosen to be 10% of full load followed by 25%, 75% and 100% of full load at regular time intervals of T=1 s.

Speed control technique proposed for DSMIM should precisely control speed with less complexity without deteriorating the performance of machine.

4.1 Open loop V/f speed control *of DSMIM*

Open loop V/f control is the most common and simple speed control method used in IMs. This method of speed control in DSMIM should maintain the synchronized dual stator voltage proportional to the frequency while achieving desired speed.

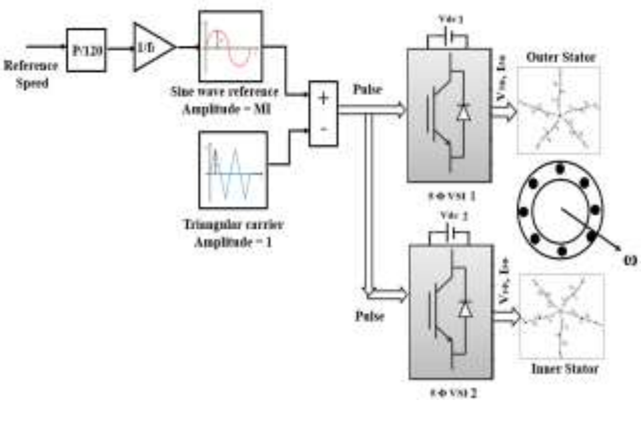

Figure 15. Simulation Block diagram of open loop V/f Controlled DSMIM

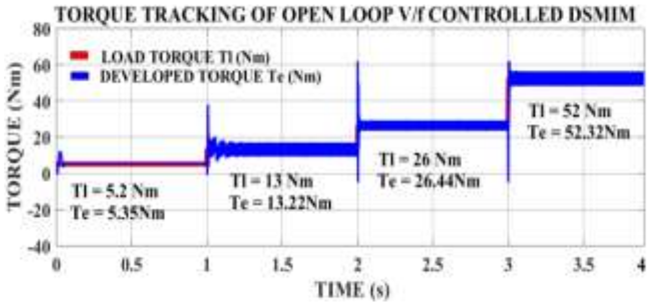

Figure 16. Torque Tracking of open loop V/f Controlled DSMIM

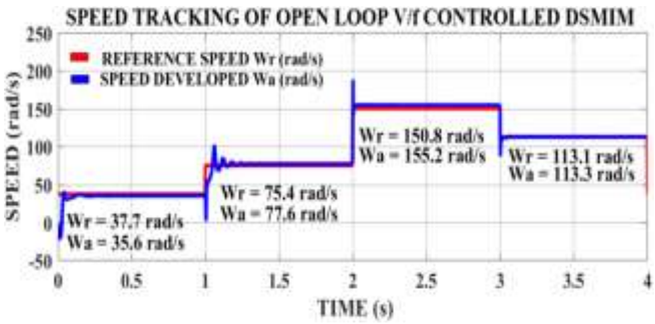

Figure 17. Speed Tracking of open loop V/f Controlled DSMIM

It is observable from Figure 16 that the developed torque signal spikes at every instant of load change. The switch over in excitation between outer and inner stator in satisfying the load demand correspondingly led to the development of high signal spikes. The developed torque tracks the load demand with a torque ripple of 23.46%. assisted. Figure 17 depicts that the actual speed tracks the reference speed at all three desired speed conditions chosen within its operating range with a steady state error less than 5%.

4.2 Closed loop V/f speed control *of DSMIM*

Closed loop V/f control for the proposed DSMIM configuration utilizes a simple PID controller that changes the frequency of the VSIs in accordance to the desired speed signal **[36]**. It also maintains a constant V/f ratio at every instant of control.

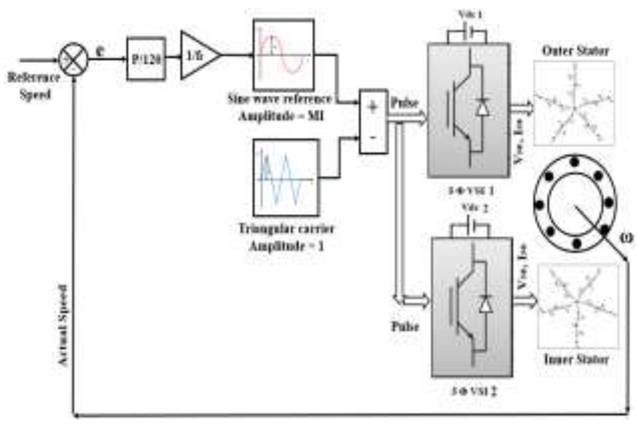

Figure 18. Simulation Block diagram of Closed Loop V/f Controlled DSMIM

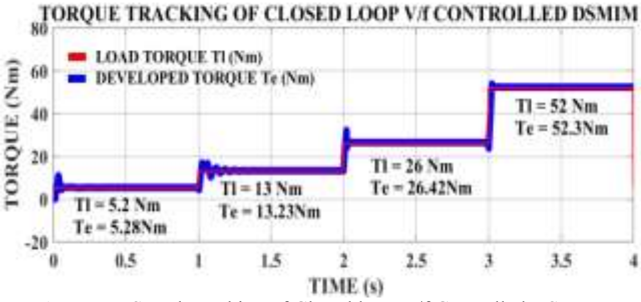

Figure 19. Speed Tracking of Closed loop V/f Controlled DSMIM

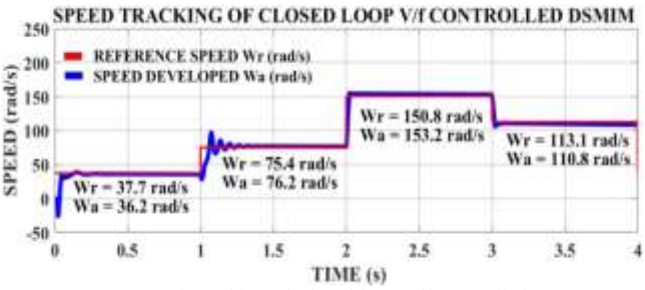

Figure 20. Speed Tracking of Closed loop V/f Controlled DSMIM

From Figure 19 it is noticeable that the developed torque tracks the load demand with a torque ripple of 6.38%.

Figure 20 depicts that the actual speed tracks the reference speed at all the three desired speed conditions within its operating range with a steady state error less than 4%.

4.3 Indirect Field Oriented Control of DSMIM

Linear characteristics of a conventional PID controller does not complement an accurate speed control action in a motor load set due to the nonlinear parameter variation during its entire operation. **[37, 38]**. Thus, this high dynamic requirement of the machine could be satisfied only by an advanced control technique that is capable of considering the non-linearity.

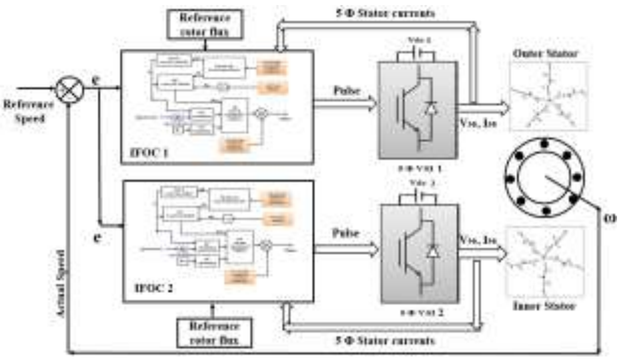

Figure 21. Simulation Block diagram of Indirect Field Oriented Controlled DSMIM

Vector Control allows a precise and wide control over speed at all four quadrants. Direct vector control methods are more advanced and respond ten times faster than indirect vector control methods but it involves flux or torque sensors that add space, complexity and cost on implementation. Considering space and cost as major constrains, implementation of a direct vector control method loses credibility in many industrial and transportation applications. IFOC scheme for induction motor grabs attention towards research due to its simplicity in implementation regardless of number of phases at the inverter to produce an n-phase stator current or voltage. It allows a very precise and rapid control of the electromechanical torque from low and zero speed conditions. Figure 21 depicts the schematics of IFOC for a dual stator five phase induction motor.

This controller model includes two conventional IFOCs and they are designed with machine parameters with respect to the outer and inner stator. The outer speed control loop is formed by reducing the error between the reference and actual speed using a PID controller. The inner current control loop involves the estimation of the reference d-q stator current by considering a constant reference rotor flux linkage. They are then compared with the actual d-q stator current sensed from the stator windings. The error between them is reduced using a hysteresis controller to generate pulse and trigger the inverter switches for the synthesis of voltage.

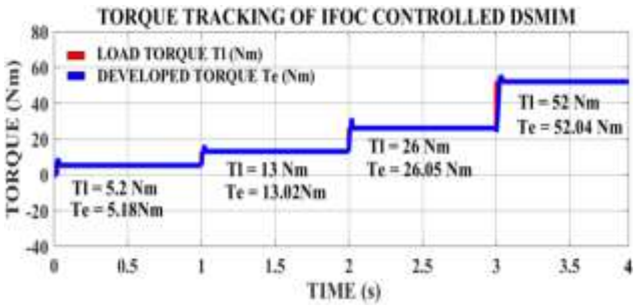

Figure 22. Torque tracking of IFOC Controlled DSMIM

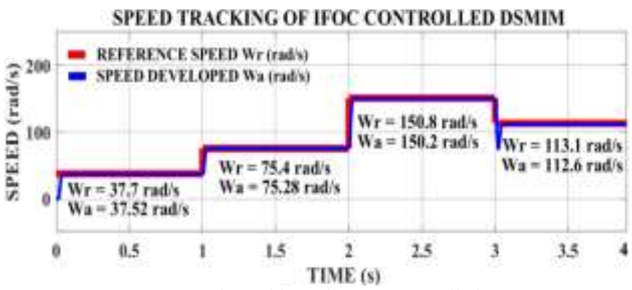

Figure 23. Speed Tracking of IFOC Controlled DSMIM

From Figure 22 it is visible that the largeness of spikes that occur at every instant of load change is curbed due to the accuracy built by IFOC. The developed torque tracks the load demand with a torque ripple of 2.47%. Figure 23 depicts that the actual speed tracks the reference speed at all the three desired speed conditions chosen within its operating range with a steady state error less than 2%.

The speed Vs torque curve for the DSMIM drive with V/f speed control and IFOC scheme are plotted and compared as shown in figure 24.

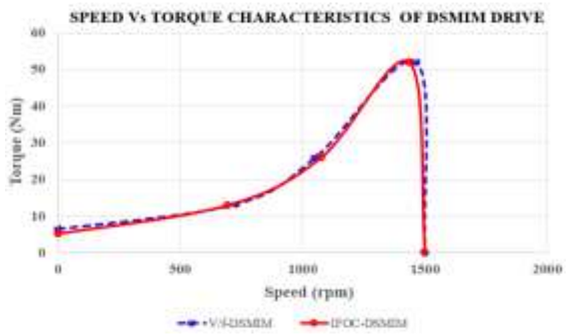

Figure 24. Speed Tracking of IFOC Controlled DSMIM

D) Single IFOC or V/f - IFOC for an EV applied DSMIM

An EV drive is anticipated to occupy less space and complexity. With this aim it is appreciable to design a single IFOC or a combination of V/f-IFOC for speed control action. In the proposed DSMIM configuration the inner stator is designed to be surrounded by the outer stator. Therefore, the dual stator's dimension and hence their parameters become non-identical. IFOC design solely depend upon the stator and rotor parameters hence it is not possible to have a single IFOC in common for dual stators of DSMIM. IFOC works precisely at low-speed operations henceforth could preferably be limited to inner stator speed control with V/f control method for the outer stator speed control. But during dual stator operation it is quite difficult to synchronize the switching frequency of the pulses developed by two different controllers. Only a synchronized switching pattern could develop a synchronized five phase voltage pattern that enhances the developed torque.

The above stated reasons rule out the ideology of using a single IFOC or a combination of V/f-IFOC for DSMIM drive.

5. Drive Cycle Testing on IFOC-DSMIM Drive

The reliability of the proposed Indirect Field Oriented Controlled DSMIM for Electric vehicle application is tested against modal drive cycle reference and transient drive cycle reference. The modal drive cycle pattern defines a protracted speed patterns that assist analysis purposes. The transient drive cycle reference defines the real time driving pattern of a vehicle. Modified Indian drive cycle (MIDC) and Highway Fuel Economy Test drive cycle (HWFET) were chosen for the speed tracking analysis under a frictional load pattern.

5.1 Modified Indian Drive Cycle

MIDC is used as a standard drive cycle in India for Type-1 test of BSIV 4 wheeled vehicles. It is mostly similar as that of the New European Driving Cycle, which is made up of four Urban Driving Cycles and an Extra-Urban driving cycle. However, the maximum speed in the MIDC has been reduced to 90 km/h considering Indian driving conditions. The torque and linear speed developed by the drive is shown in Figure 24 and Figure 25 respectively.

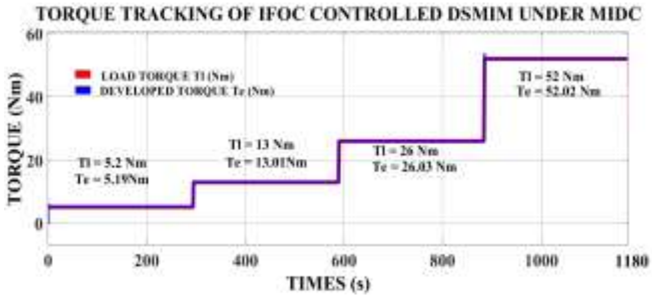

Figure 25. Torque Tracking of IFOC Controlled DSMIM under MIDC

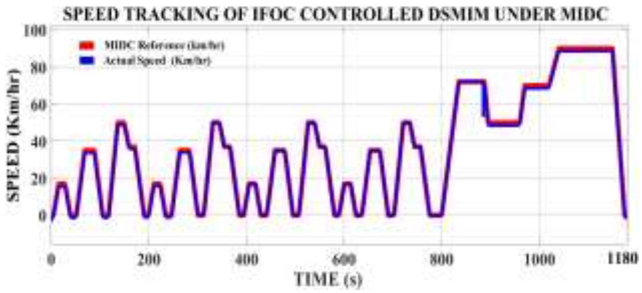

Figure 26. Speed Tracking of IFOC Controlled DSMIM under MIDC

From Figure 25 it is observable that the model develops and traces the given frictional load torque profile with a torque ripple of 1.8 %. Figure 26 depicts that the proposed drive model effectively traces the speed pattern in MIDC with a noticeable dip during braking at 890s due to the sudden raise in load.

5.2 Highway Fuel Economy Test Drive Cycle

HWFET is develop by the by the U.S. Environmental Protection Agency (U.S. EPA) for the determination of fuel economy of light duty vehicles. The maximum speed in the HWFET cycle is 90 km/h and it has no stop overs for a long duration of 765s. It covers a total distance of 16.45 km for one cycle. It is useful in the fuel economy analysis of the highway light vehicles.

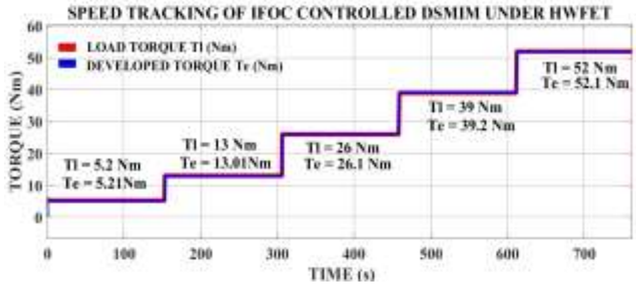

Figure 27. Torque Tracking of IFOC Controlled DSMIM under HWFET

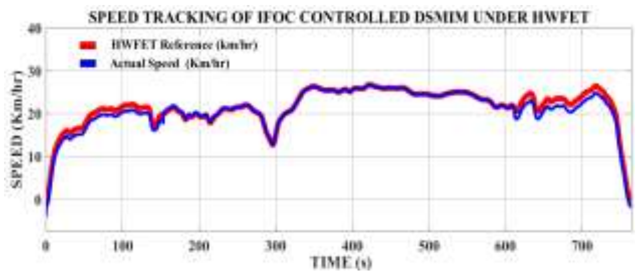

Figure 28. Speed Tracking of IFOC Controlled DSMIM under HWFET

From Figure 27 it is observable that the model develops and traces the given frictional load torque profile with a torque ripple of 1.76 %. Figure 28 depicts that the proposed drive model effectively traces the speed pattern in HWFET.

6. Conclusion

Dynamic model of DSMIM was successfully developed in MATLAB/Simulink environment. The percentage load sharing between the stators and its transient performance were studied from the free acceleration characteristics. Speed control operation of the drive is analyzed with a conventional V/f controller and a vector based IFOC controller. The speed and torque waveforms attained through the analysis were illustrated. The results depict that both V/f and IFOC controllers tracks the desired speed and torque within its operating range. The accuracy of the controllers was determined by calculating the steady state error in speed and the percentage torque ripple in developed torque. The Steady state error in speed while using a V/f controller is less than 4% and while using an IFOC controller is less than 2%. The results also exhibit that indirect Field oriented Controlled DSMIM model exhibit the advantage of lesser torque ripple with better tracking accuracy at low speed. Therefore, this model finds its importance in an EV application. It is tested against the standard MIDC and HWFET drive cycle. The model tracks the drive cycle pattern for a given frictional load profile with a steady state error of 2 %. This analysis paves way in predetermining the drive's energy efficiency under various driving patterns that supports in the erection of an effective EV system.

References

[1] W. H. Kersting, "Causes and effects of single-phasing induction motors," in *IEEE Transactions on Industry Applications*, 2005, vol. 41, no. 6, pp. 1499-1505.
[2] H. Zhong, X. Wang and Y. Pei, "Modeling and simulation of a novel high efficiency single-phase motor," *2011 6th IEEE Conference on Industrial Electronics and Applications*, 2011, pp. 1256-1259.
[3] C. B. Jacobina, M. B. De Rossiter Correa, E. R. C Da Silva, & A. M. N Lima, 'Induction motor drive system for low-power applications', IEEE Transactions on Industry Applications, 1999, vol. 35, no. 1, pp. 52-61.
[4] T. Rai and P. Debre, "Generalized modeling model of three phase induction motor," 2016 International Conference on Energy Efficient Technologies for Sustainability (ICEETS), 2016, pp. 927-931.
[5] M. Tousizadeh, H. S. Che, J. Selvaraj, N. A. Rahim and B. Ooi, "Performance Comparison of Fault-Tolerant Three-Phase Induction Motor Drives Considering Current and Voltage Limits," in IEEE Transactions on Industrial Electronics, vol. 66, no. 4, pp. 2639-2648, April 2019.
[6] Shabn J Thomas, Binbu R. "Induction Motor Based Drive for Hybrid Electric Vehicle Application" International Journal of Electrical, Electronics and Data Communication, ISSN: 2320-2084 Volume-5, Issue-7, Jul.-2017.
[7] Bindu R and Sushil Thale, Senior Member, IEEE Vashi, Navi. "Sizing of hybrid energy storage system and propulsion unit for electric vehicle", 2017 IEEE Transportation Electrification Conference.
[8] C.C. Chan and K.T. Chau, Modern Electric Vehicle Technology, Oxford University Press, New York, 2001.
[9] Chunhua Zheng, Weimin Li and Quan Liang "An Energy Management Strategy of Hybrid Energy Storage Systems for Electric Vehicle Applications", IEEE Transactions on Sustainable Energy, vol. 9, no. 4, pp. 1880-1888, Oct. 2018.
[10] C. Shi, Y. Tang and A. Khaligh, "A Three-Phase Integrated Onboard Charger for Plug-In Electric Vehicles," in IEEE Transactions on Power Electronics, vol. 33, no. 6, pp. 4716-4725, June 2018.
[11] S. A. Gaikwad and S. M. Shinde, "Review on five-phase induction motor fed by five-phase voltage source inverter with different conduction mode," International Conference on Industry 4.0 Technology (I4Tech), 2020, Pune, India, pp. 199-202.
[12] A. Dattu and M. R. Rashmi, "Modeling of five phase induction motor drive," 2017 International Conference on Technological Advancements in Power and Energy (TAP Energy), 2017, pp. 1-5.
[13] B. Jyothi, M. Venu Gopala Rao, T. Karthik "Modeling and Simulation of Five-phase Induction Motor Fed with Five-phase Inverter Topologies," 2015, Indian Journal of Science and Technology, Vol 8(19), Aug.
[14] S. K. Barik and K. K. Jaladi, "Performance characteristic of five-phase induction motor with different conduction modes in VSI," 2015, IEEE Students Conference on Engineering and Systems (SCES), pp. 1-5.
[15] W. Yu, D. Liu, J. Huang and M. Kang, "Performance analysis of multiphase induction motor drive," 2010 International Conference on Electrical and Control Engineering, 2010, pp. 5396-5400.
[16] M. Sowmiya and S. H. Thilagar, "Performance enhancement of electric vehicles using vector controlled multiphase induction motor," IEEE International Conference on Power Electronics, Drives and Energy Systems, 2018, pp. 1-6.
[17] X. Zhang, D. Gohlich and J. Li, "Energy-Efficient Toque Allocation Design of Traction and Regenerative Braking for Distributed Drive Electric Vehicles," in IEEE Transactions on Vehicular Technology, vol. 67, no. 1, pp. 285-295.
[18] A. R. Munoz and T. A Lipo, 2000, 'Dual Stator Winding Induction Machine Drive', IEEE Transactions on Industrial Applications, vol. 36, no. 5, pp. 1369-1379.
[19] Basak, S & Chakraborty, C 2015, 'Dual Stator Winding Induction Machine: Problems, Progress, and Future Scope', IEEE Transactions on Industrial Electronics, vol. 62, no. 7, pp. 4641-4652.
[20] Alberti, L & Bianchi, N 2012, 'Experimental Tests of Dual Three-Phase Induction Motor Under Faulty Operating Condition', *IEEE Transactions on Industrial Electronics*, vol. 59, no. 5, pp. 2041-2048.

[21] Bojoi, R, Tenconi, A, Griva, G & Profumo, F 2006, 'Vector Control of Dual-Three-Phase Induction-Motor Drives using Two Current Sensors', IEEE Transactions on Industry Applications, vol. 42, no. 5, pp. 1284-1292.
[22] Emmanuel Delaleau, Jean-Paul Louis & Romeo Ortega 2001, 'Modeling and control of induction motors', International Journal of Applied Mathematics and Computer Science, vol. 11, no. 1, pp. 105-129.
[23] A. Nanoty and A. R. Chudasama, "Design and control of multiphase induction motor," 2011 IEEE International Electric Machines & Drives Conference (IEMDC), 2011, pp. 354-358.
[24] G. K. Singh, K. Nam and S. K. Lim 2005, 'A Simple Indirect Field–Oriented Control Scheme for Multiphase Induction Machine', IEEE Transactions on Industrial Electronics, vol. 52, no. 4, pp. 1177-1184.
[25] Bojoi R, Farina F, Griva G, Profumo F & Tenconi A 2005, 'Direct Torque Control for Dual Three-Phase Induction Motor Drives', IEEE Transactions on Industry Applications, vol. 41, no. 6, pp. 1627-1636.
[26] Venu Gopal, BT 2017, 'Comparison between direct and Indirect Field Oriented Control of Induction Motor', International Journal of Engineering Trends and Technology, vol. 43, no. 6, pp. 364-369.
[27] Lin D and Zhou P 2008 An improved dynamic model for the simulation of three-phase induction motors with deep rotor bars. In: International Conference on Electrical Machines and Systems, Wuhan, pp. 3810-3814.
[28] Renukadevi. G and Rajambal. K, "Generalized model of multi-phase induction motor drive using MATLAB/Simulink," 2011 ISGT2011-India pp. 114-119
[29] S. Devabhaktuni and R. G., "Performance analysis of three-phase and five-phase inverters with different PWM strategies," *2019 Innovations in Power and Advanced Computing Technologies (i-PACT)*, 2019, pp. 1-5
[30] A. Iqbal, S. M. Ahmed, M. A. Khan, M. R. Khan and H. Abu-Rub, "Modeling, simulation and implementation of a five-phase induction motor drive system," 2010 Joint International Conference on Power Electronics, Drives and Energy Systems & 2010 Power India, 2010, pp. 1-6.
[31] Renukadevi, G and Rajambal, K 2012, 'Generalized d-q Model of n-Phase Induction Motor Drive,' World Academy of Science, Engineering and Technology International Journal of Electrical and Computer Engineering, Vol:6, No:9, pp.1066 – 1075.
[32] Dinesh Kumar, 2018, 'Performance Analysis of Three-Phase Induction Motor with AC Direct and VFD,' IOP Conference Series: Materials Science and Engineering, pp.1-10.
[33] Oleschuk V, Profumo F, Tenconi A, Bojoi R and Stankovic A M 2006 Synchronization of Voltage Waveforms in Basic Topologies of Dual Inverter-Fed Motor Drives. In: CES/IEEE 5th International Power Electronics and Motion Control Conference, Shanghai, China, pp.1-6
[34] Rahman, K, Rahman, S, Samiullah, M, Iqbal A & Ashraf I 2019,' V/f Control of Five-Phase Induction Motor Drive Fed from Cascaded H Bridge Multilevel Inverter,' International Conference on Electrical, Electronics and Computer Engineering (UPCON), Aligarh, India, pp. 1-5.
[35] Bojoi, R, Tenconi, A, Griva, G & Profumo, F 2006, 'Vector control of dual-three-phase induction-motor drives using two current sensors', IEEE Transactions on Industry Applications, vol. 42, no. 5, pp. 1284-1292.
[36] De Souza, TS, Bastos, RR & Cardoso Filho, BJ 2018, 'Modeling and Control of a Nine-Phase Induction Machine with Open Phases', *IEEE Transactions on Industry Applications*, vol. 54, no. 6, pp. 6576-6585.
[37] S. El Amrani, M. Chennani and D. Belkhayat, "Comparative Study of Electric Vehicle Energy Consumption between Trunk Roads and Highways," 2019 7th International Renewable and Sustainable Energy Conference (IRSEC), 2019, pp. 1-7.
[38] M. Sowmiya and S. H. Thilagar, "Performance Enhancement of Electric Vehicles using Vector Controlled Multiphase Induction Motor," 2018 IEEE International Conference on Power Electronics, Drives and Energy Systems (PEDES), 2018, pp. 1-6.

Contribution of Individual Authors to the Creation of a Scientific Article (Ghostwriting Policy)

The authors equally contributed in the present research, at all stages from the formulation of the problem to the final findings and solution.

Sources of Funding for Research Presented in a Scientific Article or Scientific Article Itself

No funding was received for conducting this study.

Conflict of Interest

The authors have no conflicts of interest to declare that are relevant to the content of this article.